An investigation of mineral dynamics in frozen seawater brines by direct measurement with synchrotron X-ray powder diffraction

Butler, B.M.; Kennedy, H.A.

Journal of Geophysical Research

DOI:
10.1002/2015JC011032

Published: 14/08/2015

Publisher's PDF, also known as Version of record

AGU PUBLICATIONS

JGR

Journal of Geophysical Research: Oceans

RESEARCH ARTICLE

10.1002/2015JC011032

Key Points:
- Novel synchrotron XRPD analysis of mineral dynamics in frozen seawater brine
- First X-ray evidence of mirabilite and hydrohalite in frozen seawater brine
- Minerals observed to interact within the frozen medium

Correspondence to:
B. M. Butler,
osu851@bangor.ac.uk

Citation:
Butler, B. M., and H. Kennedy (2015), An investigation of mineral dynamics in frozen seawater brines by direct measurement with synchrotron X-ray powder diffraction, *J. Geophys. Res. Oceans*, *120*, 5686–5697, doi:10.1002/2015JC011032.

Received 15 JUN 2015
Accepted 27 JUL 2015
Accepted article online 30 JUL 2015
Published online 14 AUG 2015

An investigation of mineral dynamics in frozen seawater brines by direct measurement with synchrotron X-ray powder diffraction

Benjamin Miles Butler[1] and Hilary Kennedy[1]

[1]School of Ocean Sciences, Bangor University, Anglesey, UK

Abstract Frozen seawater is a composite material with a sponge-like structure. The framework of the structure is composed of pure ice, and within the pores exists a concentrated seawater brine. When the temperature is reduced, the volume of this residual brine decreases, while its salinity increases. As a result of the paired changes to temperature and salinity, the brine eventually becomes supersaturated with respect to a mineral, resulting in the precipitation of microscopic crystals throughout the ice structure. Due to experimental constraints, the current understanding about the formation of these minerals relies on the analysis of the residual brine, rather than the mineral phase. Here synchrotron X-ray powder diffraction was used to assess the dynamics that occur between ice, brine, and mineral phases within frozen seawater brines that were subjected to cooling and warming at subzero temperatures. The method was able to detect crystalline phases of ice, mirabilite ($Na_2SO_4{\cdot}10H_2O$), and hydrohalite ($NaCl{\cdot}2H_2O$). Results illustrate a highly dynamic geochemical environment where ice-brine-mineral interactions tend toward an equilibrium crystallization process, which supports the process of seawater freezing that is described by the Gitterman Pathway and FREZCHEM model. This study highlights the power of synchrotron techniques in observing the mineralogical dynamics of inaccessible environmental systems.

1. Introduction

When seawater cools to its freezing point, sea ice forms, which consists of pure ice that is punctuated by brine channels and pockets that contain liquid brine and gaseous inclusions [*Golden et al*., 2007]. As the temperature of the seawater-derived brine is further decreased below its freezing point, water is again removed as a pure ice phase, the volume of the brine within the inclusions decreases and thus the salinity increases. The coupled changes in solution composition with temperature as seawater is cooled to its eutectic create a series of supersaturation events within the medium, resulting in the precipitation of a sequence of minerals.

For over a century now, the sequential process by which mineral formation occurs upon seawater freezing has been investigated [*Ringer*, 1906; *Gitterman*, 1937; *Nelson and Thompson*, 1954; *Assur*, 1960; *Marion et al*., 1999]. The current understanding of mineral dynamics within seawater-derived brines is largely based upon analysis of the changes to the major ion composition (Na^+, Cl^-, Mg^{2+}, SO_4^{2-}, Ca^{2+}, and K^+) of subzero seawater-derived brines in a laboratory setting [*Ringer*, 1906; *Gitterman*, 1937; *Nelson and Thompson*, 1954; *Assur*, 1960]. Such studies inferred the identity of the mineral precipitate by quantifying compositional changes to the brine and, where possible, identifying the minerals that formed qualitatively by use of petrographic microscopes. The two main paradigms derived from such experiments that describe the sequence of minerals that precipitate when seawater freezes are known as the Gitterman Pathway and the Ringer-Nelson-Thompson (RNT) Pathway.

The experiments carried out by Gitterman were designed to retain the minerals in contact with the brine and hence made it possible for subsequent interactions to occur between minerals and solutions as the brine composition continued to change. This pathway was characterized by the sequential onset of precipitation from the developing brine of mirabilite ($Na_2SO_4{\cdot}10H_2O$) at −7.3°C, gypsum ($CaSO_4{\cdot}2H_2O$) at −15°C, hydrohalite ($NaCl{\cdot}2H_2O$) at −22.9°C, sylvite (KCl) at −33°C, and finally $MgCl_2{\cdot}12H_2O$ at −36.2°C which is the eutectic temperature for seawater via this mineral sequence. The Gitterman experiments indicated that upon the onset of hydrohalite precipitation, mirabilite would begin to dissolve due to the creation of

undersaturated brine caused by a large reduction in Na^+. The dissolution of mirabilite consequently leads to an increase in SO_4^{2-}, resulting in conditions that enhance the precipitation of gypsum. This pathway results in equilibrium being achieved between all minerals and brine at all stages, and is therefore best likened to an equilibrium crystallization process whereby previously formed minerals are permitted to interact with the brine.

The studies that derived the RNT Pathway [*Ringer*, 1906; *Nelson and Thompson*, 1954] differed from the experimental design of Gitterman, in that at various temperatures studied, minerals were removed from the brine before further cooling, therefore preventing subsequent interaction between minerals and brine. The RNT Pathway follows a different mineral precipitation sequence to the Gitterman Pathway, with mirabilite forming at −8.2°C, hydrohalite at −22.9°C, sylvite and $MgCl_2{\cdot}12H_2O$ at −36.0°C, and a eutectic of −53.8°C which occurs upon the precipitation of antarcticite ($CaCl_2{\cdot}6H_2O$). The discrepancy of 17.6°C between the Gitterman and RNT Pathways eutectic temperatures highlights the difference in allowing for mineral interaction within the system. The RNT Pathway best represents a fractional crystallization process, which involves the removal or isolation of minerals from the system as they form [*Sha*, 2012].

FREZCHEM is a thermodynamic model that can describe the geochemistry of seawater freezing [*Marion et al*., 1999; *Marion and Kargel*, 2008; *Marion et al*., 2010]. Published material by the model's authors on the process of freezing seawater to its eutectic [*Marion et al*., 1999] uses the process of equilibrium crystallization and results in a mineral precipitation sequence that best fits the Gitterman Pathway; with the precipitation of ikaite at −2°C, mirabilite at −6.3°C, gypsum at −22.2°C, hydrohalite at −22.9°C, sylvite at −34°C, and a eutectic that occurs upon the formation of $MgCl_2{\cdot}12H_2O$ at −36.2°C.

No matter which precipitation pathway seawater undergoes when it freezes, the site of mineral precipitation in sea ice is within the brine inclusions. The dimensions and distribution of brine inclusions within the ice therefore create practical constraints for the evaluation of mineral dynamics. The brine inclusions within sea ice respond dynamically to changes in temperature, and their size decreases as the temperature is reduced because pure water is removed from the brines by the freezing of ice to the surrounding matrix in order to maintain freezing equilibrium. Therefore, minerals that form at higher temperatures, such as ikaite [*Papadimitriou et al*., 2013], have the opportunity to grow large enough (up to 600 μm) and are stable enough to allow for successful extraction by melting ice in the field [*Dieckmann et al*., 2008; *Geilfus et al*., 2013]. Successful extraction of ikaite and also gypsum from natural and experimental sea ice samples was achieved by *Geilfus et al*. [2013], who again used careful melting procedures to extract these sparingly soluble minerals. Minerals such as mirabilite and hydrohalite are estimated to be significantly smaller and too soluble to allow extraction by melting ice, and therefore have not been identified from field studies, but rather from the laboratory studies. From laboratory experiments, mirabilite crystals in sea ice have been estimated to range from 1 to 140 μm in diameter, with number densities of ∼270 crystals per mm^3 at −15°C, resulting in the mineral occupying 3% of brine volume [*Roedder*, 1984; *Light et al*., 2003]. Estimates of hydrohalite crystal size are between 1 and 1.7 μm in diameter [*Light et al*., 2003, 2004]. Qualitative observations by microphotography indicate that mirabilite crystals occupy only a fraction of the brine volume and tend to sink to the bottom of brine inclusions, whereas hydrohalite forms a heterogeneous structure with ice that is distributed throughout the brine inclusions [*Maykut and Light*, 1995; *Light et al*., 2003].

The presence of countless microscopic mineral crystals encapsulated throughout the sea ice matrix results in observable changes to the physical properties of the ice such as its tensile strength [*Assur*, 1960], and reflectivity [*Maykut and Light*, 1995; *Light et al*., 2003, 2009]. Of particular climatic interest is the effect of the mineral precipitation on the optical properties of the ice, which becomes more reflective to solar radiation as the proportion of minerals within the medium increases [*Maykut and Light*, 1995; *Light et al*., 2004]. The optical properties fundamentally control the surface albedo of sea ice and therefore contribute to climate forcings in the polar regions. For these reasons in particular, thoroughly understanding the mineral dynamics within the sea ice system is of particular relevance to our climate and the models that aim to recreate it accurately.

Given the practical constraints associated with the separation of microscopic, highly soluble minerals from sea ice during melting, coupled with that of using crystallographic techniques in the field, it is not currently feasible to carry out *in situ* crystallographic studies on sea ice within the natural environment. To obtain a better understanding of mineral precipitation, synchrotron X-ray powder diffraction (SXRPD) was utilized to study the crystallographic formation and dynamics of minerals within seawater-derived brines at subzero

temperatures. The general aim of the study was to examine the potential of the technique to identify and quantify the minerals formed *in situ* over the temperature range that sea ice experiences during the austral winter. This period is the least studied because field sites are at their most inaccessible, whilst mineral formation is likely to be most active. More particularly, we wished to investigate whether the technique could provide independent evidence of whether or not the changing structure of frozen seawater with decreasing temperature created the conditions that favor equilibrium or fractional crystallization.

2. Methods

2.1. Preparation and Analysis

Experiments designed to study mineral dynamics during the cooling and warming of sea ice were carried out on Beamline I11 (high-resolution powder diffraction) at Diamond Light Source, the UK's national synchrotron facility. The low-temperature control capabilities provided by a cryostream on Beamline I11 made it possible to replicate the conditions required for the formation of mineral precipitates in sea ice.

Experiments were carried out on concentrated seawater-derived brines in separate cooling and warming experiments. For the cooling experiment, the salinity of the brine was $S = 100$ (hereafter termed brine-100), and for the warming experiment the brine salinity was $S = 125$ (hereafter termed brine-125). These brines would be at equilibrium in sea ice at temperatures of −6.0°C and −7.7°C respectively, according to the salinity-temperature ($S_A - t$) relationship of thermally equilibrated sea ice brines, $S_A = 1000\left(1 - \frac{54.11}{t}\right)^{-1}$ [*Assur*, 1960], with S_A (in g kg^{-1}) and conductivity-based salinity (practical salinity, S) related by $S_A = 1.004715\,S$ [*Millero and Huang*, 2009]. In thermally equilibrated ice-brine systems, t represents the freezing point of brine with a salinity S_A [*Assur*, 1960]. Brine salinities were measured using a portable conductivity meter (WTW Cond 3110) with a WTW Tetracon 325 probe at laboratory temperature (20–26°C). A concentrated seawater-derived brine was used in place of seawater in order to help enhance the proportion of mineral salts that could precipitate relative to the dominant mineral phase of ice. It is important to note that using a concentrated seawater brine does not affect the mineral dynamics of the frozen seawater past its freezing point as long as the dissolved constituents of the brine are conservative relative to its salinity and the standard composition of mid-oceanic seawater [*DOE*, 1994; *Maykut and Light*, 1995]. The brines were produced via frigid concentration of filtered seawater from the School of Ocean Sciences, Bangor University. The composition of the brine was confirmed to be conservative with respect to SO_4^{2-}, Na^+, and Ca^{2+}, indicating that the solution had not been affected by the precipitation of any known mineral phase (ikaite, mirabilite, gypsum, or hydrohalite) that would be predicted by the Gitterman or RNT Pathways within the temperatures used for freezing.

Calibration of the monochromatic wavelength on Beamline I11 was made using a silicon standard (NIST 640c). For the samples, a 0.5 mm borosilicate capillary was filled with the concentrated seawater-derived brine. Data were collected at high resolution (1 mdeg steps) using the multianalyzing crystals detector array on the 2θ circle of the diffractometer. Powder patterns were obtained at a wavelength of 0.826650 Å for the cooling experiment, and 0.826404 Å for the warming experiment. Temperature was controlled by an Oxford Cryosystems Cryostream Plus with a proven temperature stability greater than 0.1°C and a working range of −193 to 227°C. Due to the small volume of brine inside the capillary, it was found that the sample had to be substantially supercooled before the solution froze.

All diffraction patterns obtained were analyzed on TOPAS v5 Academic software using the Fundamental Parameters Analysis method to obtain information on peak positions of each mineral from a Le Bail refinement. Published cell parameters were used as an initial starting point, and were allowed to refine. These values were sourced from *Fortes et al*. [2004] for ice, *Brand et al*. [2008] for mirabilite, *Klewe and Pederson* [1974] for hydrohalite, and *Boeyens and Ichharam* [2002] for gypsum. Calculated d-spacings of the hkl reflections from the refinements were used to identify peaks that were specific to each mineral.

Each experiment used only one *in situ* sample that was subjected to changing temperature, therefore the peak intensity obtained from a crystalline phase can be assumed to be proportional to its mass within the sample. For this reason, peak intensity could be used to indicate changes in mineral mass within the sample as a function of temperature [*Norish and Taylor*, 1962; *Gavish and Friedman*, 1973].

To quantify peak intensity, the three strongest reflections of mirabilite, hydrohalite, and ice (the only detectable phases) were chosen for analysis. The Miller indices and d-spacings of the chosen peaks of all three phases

Table 1. The Miller Indices and *d*-Spacing (Å) for the Mirabilite, Hydrohalite, and Ice Peaks Used in the Analysis of Peak Intensity

Mirabilite		Hydrohalite		Ice	
hkl	*d*-Spacing	*hkl*	*d*-Spacing	*hkl*	*d*-Spacing
0 2 1	4.76568	0 2 1	3.86846	0 1 2	2.67865
1 −3 −1	3.25384	2 −1 −2	2.59857	0 1 3	2.07679
0 2 3	3.19820	1 3 1	2.43683	0 1 5	1.37646

are displayed in Table 1. To aid with the calculation of peak intensity, all chosen peaks were fitted to a Gaussian distribution using the curve fitting application in Matlab R2014a [*Muñoz-Iglesias et al.*, 2013]. Peak intensity is related to its height and area (integrated intensity), both of which can be used individually as indicators of mineral mass within an *in situ* sample [*Norish and Taylor*, 1962; *Gavish and Friedman*, 1973; *Milliman and Bornhold*, 1973]. Integrated intensity was the preferred method of quantifying the strength of each peak, calculated as the product of peak height (counts) and the full width at half maximum of the peak (2θ) [*Norish and Taylor*, 1962], and was thus used for the analysis of all hydrohalite and ice peaks. The strength of the mirabilite reflections, however, was considerably lower than that of hydrohalite and ice, with the three strongest peaks having average heights that were only 4.5 ($n = 30$) and 2.3 ($n = 42$) times greater than the background of the cooling and warming experiments, respectively. Due to this relatively low signal, the mirabilite peak areas were found to be affected by background level displacement with changing temperature (Figure 1). This displacement was found to relate to the amorphous content of the sample. At −36°C when brine-125 would have been close to its eutectic, the average background level in regions of the identified mirabilite peaks was 129 counts. In comparison, when brine-125 was in purely liquid form, the average background was 213 counts. This increase was sufficient to affect the integrated intensities of mirabilite peaks used in this region and therefore peak height analysis was chosen as the more appropriate method because this parameter is affected by background displacement to a much lesser degree [*Gavish and Friedman*, 1973]. Results from the analysis of combined (sum of the three strongest reflections) peak heights (for mirabilite) and combined integrated intensities (for ice and hydrohalite) will be referred to as mass hereafter because it was assumed that relative changes in each of these parameters was representative of an absolute change in the mass of the mineral within each *in situ* sample.

2.2. Time Series

To make an initial assessment of the response of the ice-brine-mineral system to changes in temperature, two time series measurements were taken within which ice, mirabilite, and hydrohalite were identified as the only detectable minerals. First, brine-125 was cooled from ambient to −40°C and maintained at this temperature, being scanned for 5 min at various intervals over a 65 min period (Figure 2a). Second, brine-100 was cooled to −40°C for 1 h, after which it was warmed to −20°C for 50 min with a 10 min scan completed at 10, 20, and 50 min (Figure 2b). The temperature changes studied in these initial time series

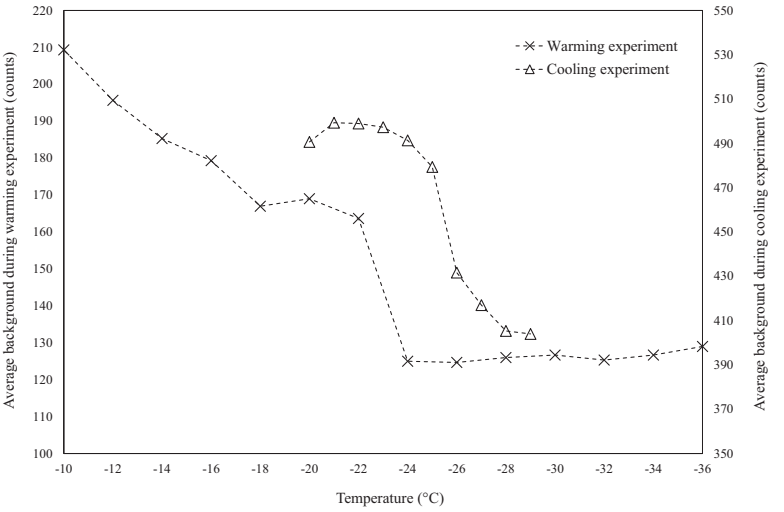

Figure 1. The fluctuations in background signal during the cooling and warming experiments, measured as an average taken from each side of the mirabilite peaks that were studied.

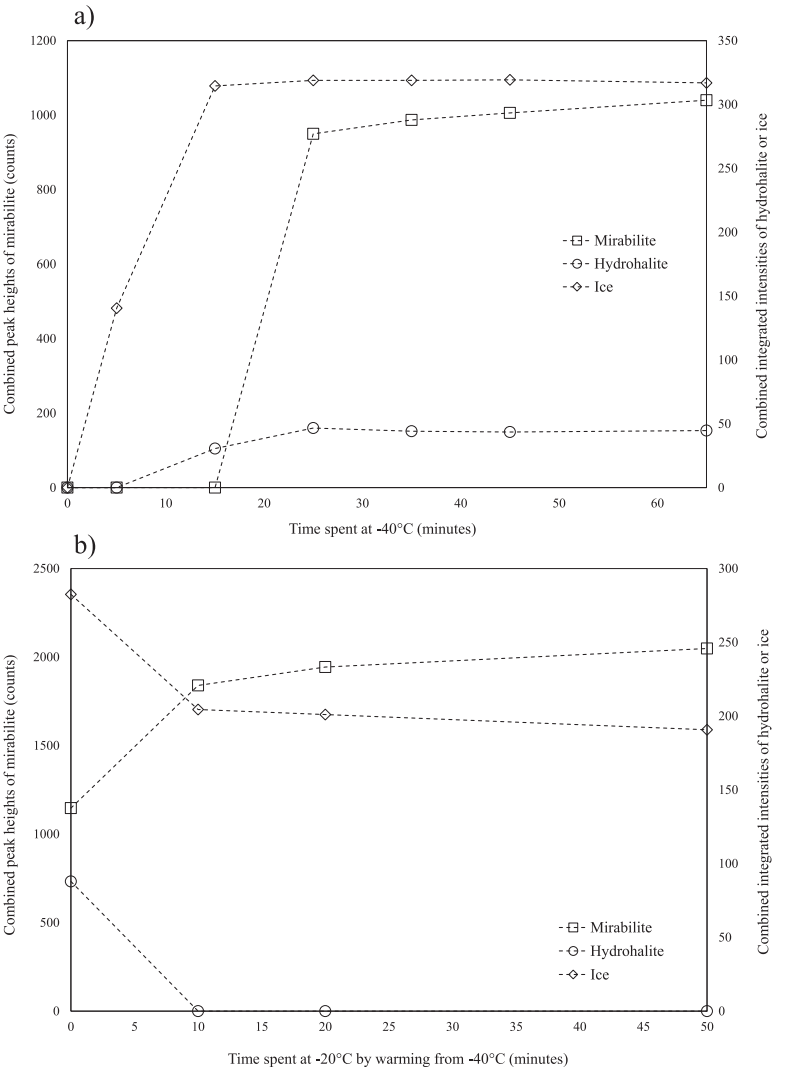

Figure 2. (a) The formation of mirabilite, hydrohalite, and ice upon cooling brine-125 from ambient to −40°C (scan time = 5 min). (b) The melting of ice, precipitation of mirabilite, and dissolution of hydrohalite upon warming brine-100 from −40 to −20°C (scan time = 10 min).

measurements were used to identify a realistic rate of change for subsequent experiments, and were at least an order of magnitude faster than the rate of temperature change used in any subsequent experiments. Although the temperature of the sample was not monitored independently, the small volume of the sample, high thermal conductivity of the capillary, and specification of the cryostream would result in a rapid response to any temperature change.

In the first time series experiment, cooling brine-125 to −40°C led to ice formation within 5 min, and hydrohalite within 15 min (Figure 2a). Both approached equilibrium after 25 min. The initial precipitation of mirabilite between 15 and 20 min was very rapid, followed by a near order of magnitude decrease in its precipitation rate after this time that continued for the remainder of the experiment.

In the second time series experiment, when the temperature of brine-100 was increased from −40°C to −20°C, all phases responded to the temperature change in the first 10 min with hydrohalite completely dissolving, while ice mass decreased and mirabilite mass increased rapidly (Figure 2b). For the subsequent 40 min, ice continued melting while mirabilite continued to precipitate at a much slower rate.

The results of the time series experiments indicated that, with a rapid and large change in temperature, either warming or cooling, equilibrium for ice and hydrohalite was approached within 25 min. Mirabilite formation, however, which is reported to have slow kinetics [*Weeks*, 2010], may not have reached equilibrium.

It should be noted that the time series experiments are not representative of the natural rates of temperature change that sea ice may be subjected to, and were rather used to inform the time required in subsequent experiments to ensure that a reasonable approximate for equilibrium conditions was used in subsequent cooling and warming experiments.

2.3. Cooling and Warming Experiment Protocol

In response to the time series results, the subsequent experiments employed small (1–2°C) incremental temperature changes and longer periods at temperature of between 25 min and 1 h that are more representative of diurnal changes that sea ice may experience in the austral winter. First, brine-100 was maintained at −20°C for 50 min before cooling in 1°C increments from −20 to −29°C. The cooled sample was maintained at each temperature for 30 min before a 30 min scan. Second, brine-125, that had been cooled and maintained at −36°C for 45 min, was subsequently warmed in 2°C increments to −10°C. The warmed sample was maintained at each temperature for 5 min before a 20 min scan. The protocols will be referred to separately as the cooling and warming experiments hereafter.

3. Results

In the cooling experiment, the mass of mirabilite increased as brine-100 was cooled from −20 to −24°C, indicating that the chemically evolving composition of the brine was sustaining its supersaturation with respect to mirabilite (Figure 3a). As the temperature was lowered beyond −24°C the mirabilite mass decreased, indicating that the brine became undersaturated with respect to this mineral, resulting in dissolution. The onset of mirabilite dissolution coincided with the first detectable sign of hydrohalite at −25°C. The mass of hydrohalite then continued to increase rapidly below −25°C, showing that the brine sustained supersaturation with respect to hydrohalite until the experiment was terminated at −29°C. Between −24 and −27°C there was a substantial increase in ice mass (Figure 3b). The rate of ice formation reduced toward −29°C when the experiment was terminated. The sharp increase in ice mass between −24 and −27°C coincided with the precipitation of hydrohalite and dissolution of mirabilite (Figure 3a). The observed trends in ice formation represent a dynamic balance between the temperature, brine composition, and water removal into the hydration waters of mirabilite and hydrohalite.

In the warming experiment, as brine-125 was warmed from −36 to −26°C, the mass of hydrohalite showed a decreasing trend, while that of mirabilite increased, indicating that the brine was gradually becoming undersaturated with respect to hydrohalite but increasingly supersaturated with respect to mirabilite (Figure 4a). On further warming above −26°C, the mass of hydrohalite decreased rapidly, resulting in total dissolution by −22°C. Between −22 and −10°C, only mirabilite remained, with an increasingly rapid decline in its mass at temperatures warmer than −14°C. Ice mass upon warming brine-125 from −36 to −10°C displayed two nearly linear periods of decrease separated by an accelerated drop in the ice mass which coincided with the temperature for complete dissolution of hydrohalite between −22 and −24°C (Figure 4b).

4. Discussion

4.1. Detected Minerals

Taking all experiments into account, temperatures ranged from −10 to −40°C. According to the given pathways for seawater freezing (Gitterman, RNT, and FREZCHEM), this temperature range could include the precipitation of ikaite, mirabilite, gypsum, hydrohalite, sylvite, and $MgCl_2{\cdot}12H_2O$. In our study, ice, mirabilite, and hydrohalite were the only crystalline phases detected.

During the formation of sea ice, the reduction in temperature and increased salinity of the brine results in a raised pCO_2 and reduced pH [*Geilfus et al*., 2014; *Papadimitriou et al*., 2014]. These conditions, recreated in our experimental runs, would not be expected to precipitate ikaite due its raised solubility [*Papadimitriou et al*., 2013].

Successful detection of any mineral in our experiments is largely determined by its mass within the sample, which itself is dictated by the initial composition of the seawater/brine, and the number of hydration waters that are incorporated into the mineral. The FREZCHEM model predicts (with ikaite excluded) that the eutectic of seawater will occur at −36.2°C after the precipitation of five minerals in different

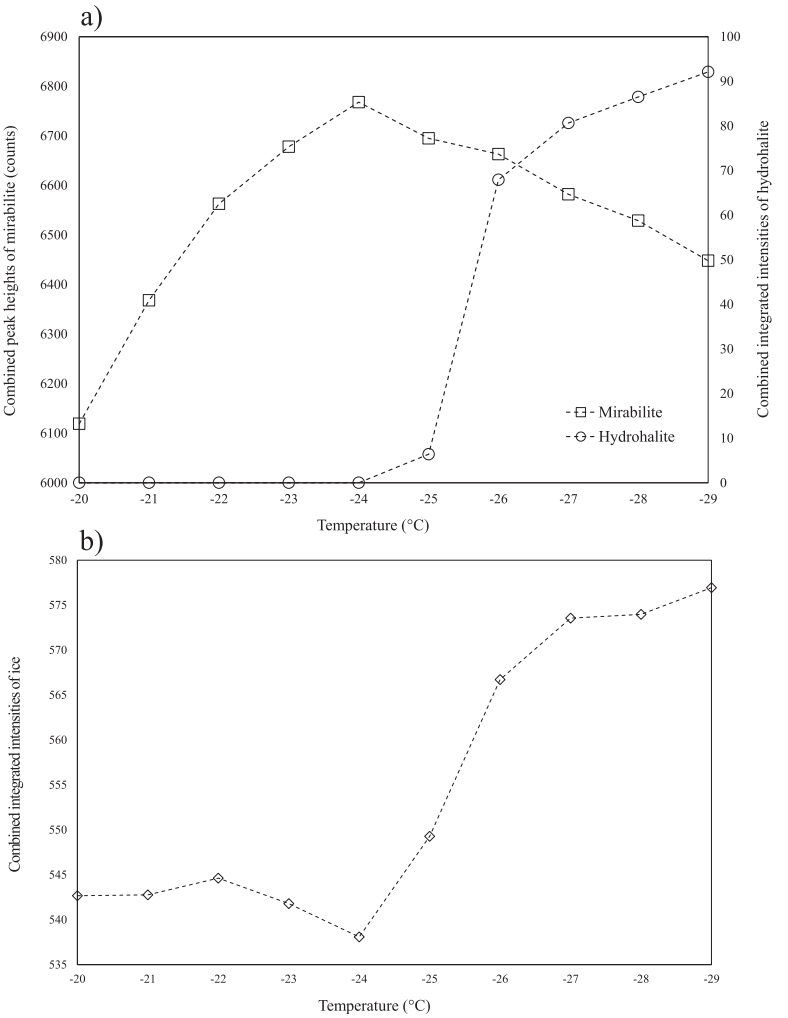

Figure 3. Cooling experiment: (a) the change in combined peak heights of mirabilite and integrated intensities of hydrohalite within brine-125 as it was cooled from −20 to −29°C. (b) The change in combined integrated intensities of ice within brine-125 as it was cooled from −20 to −29°C.

proportions (Figure 5). Given that the mass of mirabilite within the samples was approaching the detection limit of the method, indicated by the susceptibility of the signal to background displacement (Figure 1), it is likely that gypsum and sylvite would have been undetectable due to their relatively low concentrations (3 and 29 times lower than mirabilite, respectively). In contrast, $MgCl_2{\cdot}12H_2O$ is predicted to precipitate in quantities approximately triple that of mirabilite, and therefore should have been detected a temperatures below −36.2°C. The absence of any peaks that can be attributed to $MgCl_2{\cdot}12H_2O$ throughout our experiments therefore could be accounted for by other factors, such as the possibility of supercooling at the eutectic [*Toner et al*., 2014], or insufficient equilibration/scan time/replication at temperatures below −36.2°C (which was only reached during the time series experiment at −40°C, Figure 2a). In either case, further experiments specifically designed to assess the mineral dynamics at temperatures approaching and below the eutectic of seawater would be required to define and explain the absence of $MgCl_2{\cdot}12H_2O$.

Despite the absence of several minerals from the cooling and warming experiments, the detected minerals of mirabilite and hydrohalite are likely to be the most abundant minerals in sea ice throughout the temperatures at which it exists in the environment, and are the most influential in controlling the optical properties of sea ice [*Light et al*., 2004, 2009; *Ebert and Curry*, 1993]. Therefore, new evidence detailing their dynamics within the sea ice system is of particular relevance to the polar environments on Earth.

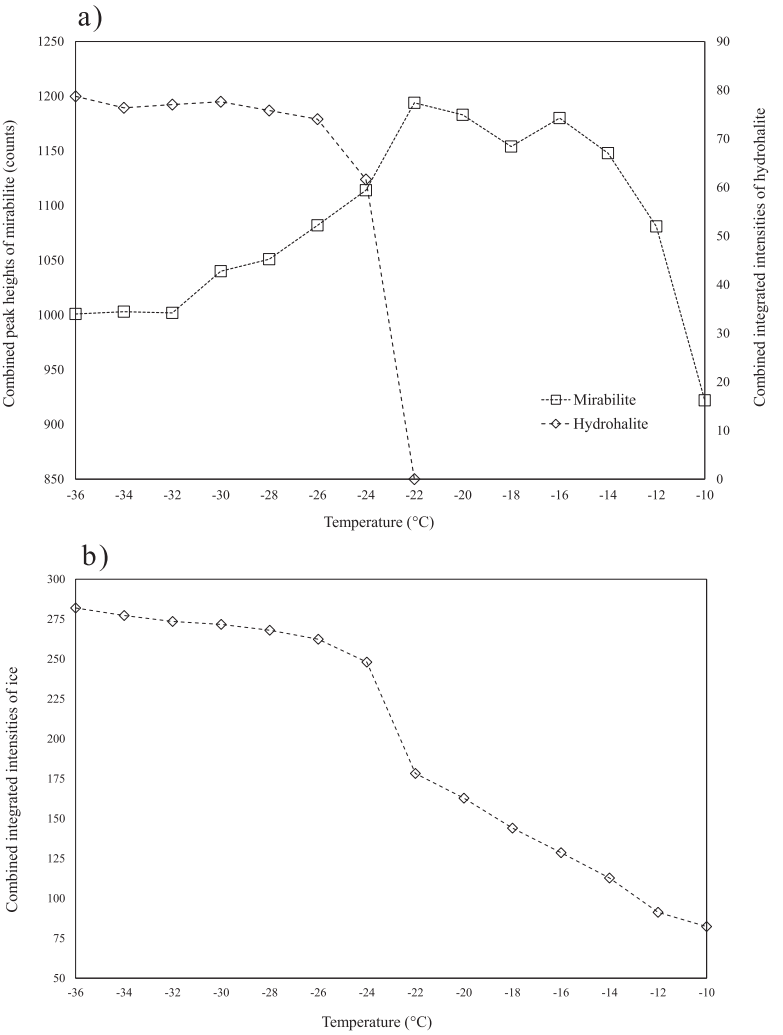

Figure 4. Warming experiment: (a) the change in combined peak height of mirabilite and combined integrated intensity of hydrohalite when brine-125 as was warmed from −36 to −10°C. (b) The change in average integrated intensity of ice when brine-125 was warmed from −36 to −10°C.

4.2. Mirabilite and Hydrohalite Interaction

This study represents a novel method which utilizes *in situ* SXRPD to unequivocally identify the mirabilite and hydrohalite dynamics within sea ice as the ambient temperature is lowered and raised. The results are the first direct X-ray evidence of mirabilite and hydrohalite presence within frozen seawater brines which can be related to their existence in natural sea ice within the temperature range studied. The technique also provides insights of how the environmental setting within the brine pockets affects mineral dynamics. Whether minerals, once formed, are isolated from the brine preventing any further interaction with the fluid or not has important implications for the proposed pathways by which freezing seawater takes to its

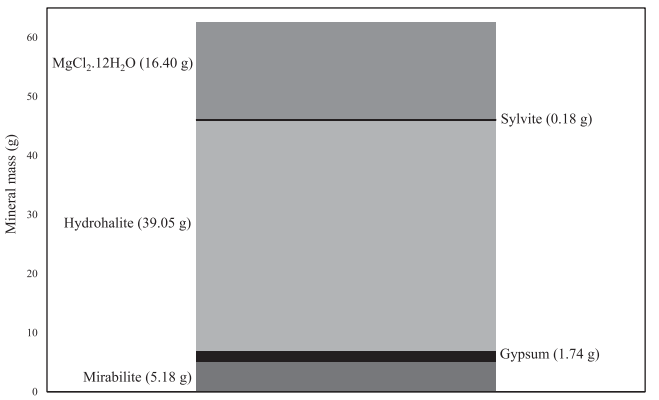

Figure 5. FREZCHEM predictions of the precipitated mineral assemblage from freezing seawater ($S = 35$) to its eutectic at −36.2°C.

eutectic, and prior to this study had never been investigated [*Gitterman*, 1937; *Nelson and Thompson*, 1954; *Marion et al*., 1999].

The cooling experiment showed mirabilite mass increasing between −20 and −24°C; a result of the coupled effect of decreasing solubility with lower temperature, and the higher Na^+ and SO_4^{2-} concentration as the brine salinity increases (Figure 3a). Such a trend in mirabilite's solubility with decreasing temperature in sea ice would be expected [*Vavouraki and Koutsoukos*, 2012; *Marion et al*., 1999]. Instead of a continued increase in mass, mirabilite started to dissolve below −24°C, coincident with the temperature at which hydrohalite was first detected. Our results are consistent with the changes proposed by *Gitterman* [1937] and *Marion et al*. [1999] that the concentrations of Na^+ and SO_4^{2-} in the brine are controlled by mirabilite precipitation until the brine becomes supersaturated with respect to hydrohalite. Either the degree of supersaturation of hydrohalite is higher than that of mirabilite or the kinetics of hydrohalite precipitation is faster, but the result is that the reduction in dissolved Na^+ concentration causes undersaturation of the brine with respect to mirabilite and its dissolution. Mirabilite dissolution will then result in an increase of dissolved SO_4^{2-} in the residual brine.

The warming experiment, which presents data over a wider temperature range, confirms the relative changes in mirabilite and hydrohalite mass (Figure 4a). As the temperature warmed from −36°C, the trend seen in the cooling experiment is reversed as hydrohalite dissolves, releasing excess Na^+ into the residual brine and leading to supersaturation and precipitation of mirabilite. At −22°C, the onset of mirabilite dissolution coincides with the complete dissolution of hydrohalite, driven by the increased solubility of mirabilite at higher temperatures in less saline brines, and the absence of any further hydrohalite dissolution acting as a source of Na^+.

The changes observed *in situ* during the cooling and warming experiments differ from the results of experiments used to derive the RNT pathway for seawater freezing, which employed a methodology that enforced fractional crystallization (FC). The changes are however consistent with the concept of equilibrium crystallization (EC) described by the Gitterman Pathway and FREZCHEM model. FC processes were proposed to be characteristic of samples that are cooled quickly [*Zolotov and Shock*, 2001], resulting in separation of a mineral from the surrounding matrix [*Weeks*, 2010]. It is therefore surprising to find evidence of EC, within the rapidly cooled samples that were analyzed in these experiments. The observation of mineral interaction within our samples implies that mirabilite and hydrohalite were present together in the brine pockets, and that changes in the saturation state of one of the minerals resulted in a direct and opposite effect on the other.

Despite results supporting the equilibrium crystallization paradigms described by the Gitterman Pathway and FREZCHEM model with respect to mirabilite and hydrohalite, there is a distinct difference that concerns the precipitation of gypsum. The Gitterman Pathway predicts the onset of gypsum precipitation at −15°C, while the FREZCHEM model predicts the onset to occur at −22.2°C before being further fueled by equilibrium reactions between hydrohalite and mirabilite below −22.9°C. Furthermore, gypsum crystals have recently been detected in laboratory and experimental sea ice [*Geilfus et al*., 2013]. Gypsum was not detected in any sample analyzed throughout either the cooling or warming experiment presented here, which as already outlined, may be due to the detection limit of the method. Aside from the limit of detection, there are two further reasons that could help explain the absence of gypsum: (1) gypsum did not precipitate within our samples; (2) the brines were supersaturated with respect to gypsum, but the mineral did not precipitate due to slow kinetics [*Weeks*, 2010; *Reznik et al*., 2009].

The solubility of gypsum in the subzero seawater-derived brines that exist in sea ice has never been determined, and it may therefore be feasible that in the conditions studied, brine-100 and brine-125 never became supersaturated with respect to gypsum.

The FREZCHEM model and Gitterman Pathway predict gypsum precipitation under the conditions used in this study. The FREZCHEM model is, however, based on equilibrium thermodynamics and therefore does not account for the rate at which chemical reactions occur. Furthermore, the Gitterman pathway is based on experiments that lasted up to 4 weeks, much longer than our study. It is possible that the short time scale employed here did not allow sufficient time for gypsum precipitation. To assess the importance of kinetic control on gypsum precipitation using X-ray crystallography would therefore require a long duration *in situ* experiment. Furthermore, measuring the solubility of gypsum within subzero seawater-derived brines

would aid in resolving gypsum dynamics in sea ice, and help to explain the source of gypsum crystals that were observed in sea ice by *Geilfus et al*. [2013].

The final implication of the mineral dynamics observed in our experiments concerns the precipitation/dissolution of hydrohalite, and this mineral's sensitivity to temperature changes. The amount of light scattering that sea ice exhibits has been shown to increase substantially between −24 and −30°C due to the precipitation of hydrohalite [*Light et al*., 2004], giving its presence climatic implications for the feedback mechanisms associated with the high albedo of sea ice [*Light et al*., 2009; *Ebert and Curry*, 1993]. Any change in the temporal or spatial extent of sea ice experiencing low atmospheric temperatures (<−23°C), or a general warming of minimum winter temperatures may therefore have a significant impact given the sensitivity of hydrohalite solubility between −22 and −25°C detected in this study. On a more practical level, despite hydrohalite being the most abundant mineral phase in cold sea ice, this sensitivity to temperature and small crystal size (<1.7 μm) [*Light et al*., 2004] combine to make it unlikely that hydrohalite crystals could ever be extracted from an environmental sample by melting procedures such as those used by *Dieckmann et al*. [2008] and *Geilfus et al*. [2013].

4.3. Ice Dynamics

The rates of change in ice mass from the cooling and warming experiments (Figures 3b and 4b) provide novel crystallographic data on the way that seawater approaches its eutectic. In both the cooling and warming experiments, there was a sharp increase in ice formation/melt that coincided with the precipitation/dissolution of hydrohalite, indicating that the behavior of the ice and hydrohalite are interlinked by associated changes in brine composition.

The ice data from the warming experiment displayed less variability than that of the cooling experiment. This difference could reside from the observation of how brines approaching their eutectic can often become supercooled [*Toner et al*., 2014], but the reverse cannot apply. Although a supercooled brine exists in a thermodynamically unstable state, the phenomenon is observed because crystal nucleation requires the energy intensive process of the formation of an interface between a crystal surface and surrounding solution. This energy is provided by the solution becoming supersaturated (which in the case of freezing seawater would require supercooling) to a point at which the free energy exceeds the energy required for the formation of a stable nucleus upon which the crystal can grow [*Toner et al*., 2014]. If supercooling occurred within our samples, the process could also result in a delayed onset for the precipitation of minerals because there would be no ionic change in solution composition as temperature decreased. Although there is a slight discrepancy between the temperature of precipitation/dissolution for hydrohalite from the cooling and warming experiments (the precipitation of hydrohalite occurred >1°C cooler than expected from all known predictions), we are unable to infer as whether the observation is due to supercooling with respect to ice, or supersaturation of the brine with respect to hydrohalite.

The results are the first direct X-ray evidence consistent with a change in rate of ice formation and melt that coincides with the precipitation or dissolution of hydrohalite respectively. The evidence of a hydrohalite-ice interaction within the *in situ* samples confirms that precipitation or dissolution of hydrohalite affects the freezing point of the brine within the sample, which is governed by its salinity/ionic strength. The ionic constituents of hydrohalite, Na^+ and Cl^-, are the most concentrated solutes within seawater; comprising 86% of the mass of salt in conservative seawater/brine [*DOE*, 1994]. The FREZCHEM model indicates (from a starting salinity, $S = 35$) that 35.2 g hydrohalite/kg frozen seawater is precipitated when the temperature reaches −29°C. The precipitation of hydrohalite removes Na^+ and Cl^- from solution, and at the same time removes pure water to form hydration waters. The overall effect of hydrohalite precipitation on the brine salinity is therefore a balance between the removal of dissolved constituents and water. Precipitation of 35.2 g of hydrohalite between −23 and −29°C from 1 kg of seawater equates to the removal of 13.4 g H_2O and 21.8 g NaCl, which is equal to a 14.3% reduction in water within the frozen system, and a 71.2% reduction in the salt content by mass. The overall effect of hydrohalite precipitation on the residual brine is therefore a reduced ionic strength that elevates the freezing point, and promotes the formation of ice.

Outputs from the FREZCHEM model (version 15.1 run in equilibrium mode between −10 and −36°C with a starting composition identical to the standard composition of mid oceanic seawater [*DOE*, 1994]) showed a similar trend to our observed dynamics of ice (Figure 6). In comparison, if hydrohalite is disabled from the model, there is no significant change in the rate of ice formation at the point of hydrohalite precipitation.

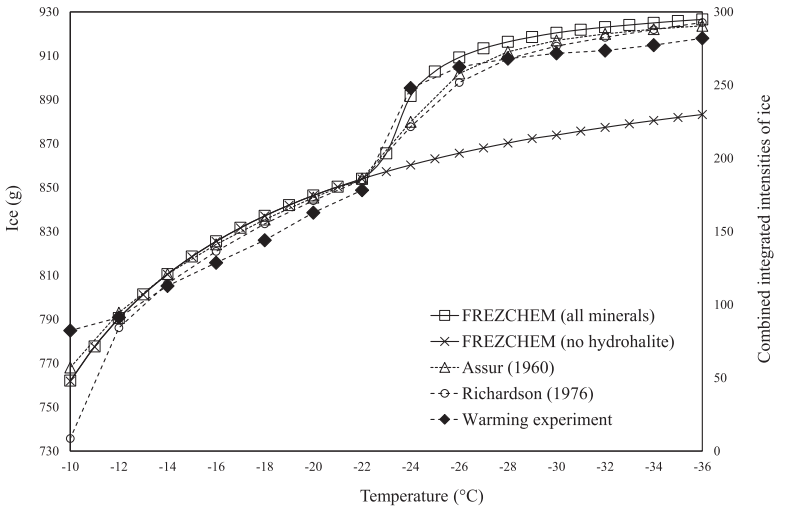

Figure 6. The change in ice content upon freezing 1 kg of seawater ($S = 35$) between −10 and −36°C. The data of water content (g) given by *Richardson* [1976] were converted to an estimate of ice content by accounting for the published quantities of mineral mass at each temperature. "FREZCHEM (all minerals)" represents the output obtained when the FREZCHEM model was run with all mineral phases enabled. "FREZCHEM (no hydrohalite)" represents the output obtained when the FREZCHEM model was run with all minerals other than hydrohalite enabled. Results from the warming experiment are plotted on a secondary *y* axis to enable comparison of trends between our observed values and mass measurements.

The FREZCHEM model therefore predicts that between −23 and −28°C, the precipitation of hydrohalite induces the formation of an extra 48.42 g of ice. Other runs of the model that excluded the precipitation of mirabilite, gypsum, and sylvite, resulted in no discernable change in the rate of ice formation.

Experimental measurements of ice content during seawater freezing from *Assur* [1960] and [*Richardson*, 1976] are also displayed in Figure 6, and show strong agreement with FREZCHEM. Between −22 and −26°C the collated data display an average ($\pm 1\sigma$) increase in the rate of ice formation that is 269 ± 55% greater than the rate between −18 and −22°C. The trends in ice data are best compared to changes observed in the warming experiment (plotted on a secondary *y* axis, Figure 6), which displays a rate of change between −22 and −26°C that is of 246% larger than that between −18 and −22°C. The similarity, in both trends and rates, between the data from our experiment and that from traditional studies and model predictions, substantiates the *in situ* method used here as a reliable and reproducible technique for studying inaccessible geochemical environments at subzero temperatures.

5. Conclusions

Our study provides the first direct X-ray evidence of mirabilite and hydrohalite in frozen seawater brines, the dynamics of which can be extrapolated to highlight the behavior of these minerals in much of the sea ice on Earth. The results importantly highlight the use of *in situ* synchrotron techniques for studying the geochemistry of inaccessible environments at low temperatures. Specifically, results from both cooling and warming seawater-derived brines at subzero temperatures suggest that mineral precipitation occurs via a process that is best described as an equilibrium crystallization pathway where minerals are allowed to interact. The process is therefore best predicted by the work of *Gitterman* [1937] and the FREZCHEM model. The four-way ice-brine-mirabilite-hydrohalite interactions within the frozen matrix highlighted here make for a highly dynamic geochemical environment that would be impossible to study crystallographically at present without *in situ* laboratory techniques. Much longer duration experiments, such as those proposed by the new facility at Diamond (Beamline I11 LDE), would allow for a more detailed examination of the seasonal changes in mineral composition within the ice and would be more representative of equilibrium conditions. Further testing at temperatures approaching the eutectic of seawater would aid in elucidating the dynamics of $MgCl_2{\cdot}12H_2O$. The experiment has highlighted the sensitivity of hydrohalite to temperature changes, which is important for the possibility of its physical separation from sea ice in the field, and also with respect to its effect on the reflectivity of sea ice; highlighting how changes in winter temperatures may affect and the surface albedo via hydrohalite dynamics within the system.

Acknowledgments
The work was supported by a NERC Algorithm Studentship (NE/K501013) and beamtime awards EE-6847 and EE-3897 from Diamond Light Source Ltd. We are very thankful to the I11 beamline team, Tang, and Murray for their support during beamtime and with data analysis. We also thank two anonymous reviewers for their helpful comments and suggestions. All data presented here are freely available upon contacting the corresponding author.

References

Assur, A. (1960), Composition of sea ice and its tensile strength, technical report 44, Arctic Sea Ice, U.S. National Academy of Sciences, National Research Council, U.S.A.

Boeyens, J. C. A., and V. V. H. Ichharam (2002), Redetermination of the crystal structure of calcium sulphate dihydrate, $CaSO_4{\cdot}2H_2O$, *Z. Kristallogr.*, *217*, 9–19.

Brand, H. E. A., A. D. Fortes, I. G. Wood, K. S. Knight, and L. Vočadlo (2008), The thermal expansion and crystal structure of mirabilite ($Na_2SO_4{\cdot}10D_2O$) from 4.2 to 300 K, determined by time-of-flight neutron powder diffraction, *Phys. Chem. Miner.*, *36*(1), 29–46.

Dieckmann, G. S., G. Nehrke, S. Papadimitriou, J. Göttlicher, R. Steininger, H. Kennedy, D. Wolf-Gladrow, and D. N. Thomas (2008), Calcium carbonate as ikaite crystals in Antarctic sea ice, *Geophys. Res. Lett.*, *35*, L08501, doi:10.1029/2008GL033540.

DOE (1994), *Handbook of Methods for the Analysis of the Various Parameters of the Carbon Dioxide System in Sea Water*, Version 2, edited by A. G. Dickson and C. Goyet, ORNL/CDIAC.

Ebert, E., and J. Curry (1993), An intermediate one-dimensional thermodynamic sea ice model investigation ice-atmosphere interactions, *J. Geophys. Res.*, *98*(C6), 10,085–10,109.

Fortes, A. D., I. G. Wood, D. Grigoriev, M. Alfredsson, S. Kipfstuhl, K. S. Knight, and R. I. Smith (2004), No evidence for large-scale proton ordering in Antarctic ice from powder neutron diffraction, *J. Chem. Phys.*, *120*(24), 11,376–11,379.

Gavish, E., and G. M. Friedman (1973), Quantitative analysis of calcite and Mg-calcite by X-ray diffraction: Effect of grinding on peak height and peak area, *Sedimentology*, *20*, 437–444.

Geilfus, N.-X., R. J. Galley, M. Cooper, N. Halden, A. Hare, F. Wang, D. H. Søgaard, and S. Rysgaard (2013), Gypsum crystals observed in experimental and natural sea ice, *Geophys. Res. Lett.*, *40*, 6362–6367, doi:10.1002/2013GL058479.

Geilfus, N.-X., J.-L. Tison, S. F. Ackley, S. Rysgaard, L. A. Miller, and B. Delille (2014), Sea ice pCO_2 dynamics and air-ice CO_2 fluxes during the Sea Ice Mass Balance in the Antarctic (SIMBA) experiment—Bellinghausen Sea, Antarctica, *Cryosphere*, *8*, 2395–2407.

Gitterman, K. E. (1937), Thermal analysis of sea water, technical report CRREL TL287. USA Cold Reg. Res. Eng. Lab., Hanover, N. H.

Golden, K. M., H. Eicken, A. L. Heaton, J. Miner, D. J. Pringle, and J. Zhu (2007), Thermal evolution of permeability and microstructure in sea ice, *Geophys. Res. Lett.*, *34*, L16501, doi:10.1029/2007GL030447.

Klewe, B., and B. Pederson (1974), The crystal structure of sodium chloride dihydrate, *Acta Crystallogr., Sect. B Struct. Crystallogr. Cryst. Chem.*, *30*, 2363–2371.

Light, B., G. A. Maykut, and T. C. Grenfell (2003), Effects of temperature on the microstructure of first-year Arctic sea ice, *J. Geophys. Res. 108*(C2), 3051, doi:10.1029/2001JC000887.

Light, B., G. A. Maykut, and T. C. Grenfell (2004), A temperature-dependent, structural-optical model of first-year sea ice, *J. Geophys. Res.*, *109*, C06013, doi:10.1029/2003JC002164.

Light, B., R. E. Brandt, and S. G. Warren (2009), Hydrohalite in cold sea ice: Laboratory observations of single crystals, surface accumulations, and migration rates under a temperature gradient, with application to 'Snowball Earth', *J. Geophys. Res.*, *114*, C07018, doi:10.1029/2008JC005211.

Marion, G. M., and J. S. Kargel (2008), *Cold Aqueous Planetary Geochemistry With FREZCHEM*, Springer, Heidelberg, Germany.

Marion, G. M., R. E. Farren, and A. J. Komrowski (1999), Alternative pathways for seawater freezing, *Cold Reg. Sci. Technol.*, *29*, 259–266.

Marion, G. M., M. V. Mironenko, and M. W. Roberts (2010), FREZCHEM: A geochemical model for cold aqueous solutions, *Comput. Geosci.*, *36*, 10–15.

Maykut, G., and B. Light (1995), Refractive-index measurements in freezing sea-ice and sodium chloride brines, *Appl. Opt.*, *34*(6), 950–961.

Millero, F. J., and F. Huang (2009), The density of seawater as a function of salinity (5 to 70 g kg^{-1}) and temperature (273.15 to 363.15 K), *Ocean Sci.*, *5*(2), 91–100.

Milliman, J. D., and B. D. Bornhold (1973), Peak height versus peak intensity analysis of X-ray diffraction data, *Sedimentology*, *20*, 445–448.

Muñoz-Iglesias, V., L. Bonales, and O. Prieto-Ballesteros (2013), pH and salinity evolution of Europa's brine: Raman spectroscopy study of fractional precipitation at 1 and 300 bar, *Astrobiology*, *13*(8), 693–702.

Nelson, K. H., and T. G. Thompson (1954), Deposition of salts from sea water by frigid concentration, technical report 29, Off. Naval Res., Arlington, Va.

Norish, K., and R. Taylor (1962), Quantitative analysis by X-ray diffraction, *Clay Miner. Bull.*, *5*(28), 98–109.

Papadimitriou, S., H. Kennedy, P. Kennedy, and D. N. Thomas (2013), Ikaite solubility in seawater-derived brines at 1 atm and sub-zero temperatures to 265 K, *Geochem. Cosmochim. Acta*, *109*, 241–253.

Papadimitriou, S., H. Kennedy, P. Kennedy, and D. N. Thomas (2014), Kinetics of ikaite precipitation and dissolution in seawater-derived brines at sub-zero temperatures to 265 K, *Geochem. Cosmochim. Acta*, *140*, 199–211.

Reznik, I. J., I. Gavrieli, and J. Ganor (2009), Kinetics of gypsum nucleation and crystal growth from Dead Sea brine, *Geochem. Cosmochim. Acta*, *73*(20), 6218–6230.

Richardson, C. (1976), Phase relationships in sea ice as a function of temperature, *J. Glaciol.*, *17*(77), 507–519.

Ringer, W. E. (1906), De varanderingon in samenstelling van zeewater bij het bevriezen, *Chem. Weekblack*, *3*, 223–249.

Roedder, E. (1984), Fluid inclusions, *Rev. Mineral.*, *12*, 1–646.

Sha, L. K. (2012), Concurrent fractional and equilibrium crystallisation, *Geochem. Cosmochim. Acta*, *86*, 52–75.

Toner, J., D. Catling, and B. Light (2014), The formation of supercooled brines, viscous liquids, and low-temperature perchlorate glasses in aqueous solutions relevant to Mars, *Icarus*, *233*, 36–47.

Vavouraki, A. I., and P. G. Koutsoukos, (2012), Kinetics of crystal growth of mirabilite in aqueous supersaturated solutions, *J. Cryst. Growth*, *338*(1), 189–194.

Weeks, W. (2010), *On Sea Ice*, Univ. of Alaska Press, Fairbanks.

Zolotov, M. Y., and E. L. Shock (2001), Composition and stability of salts on the surface of Europa and their oceanic origin, *J. Geophys. Res.*, *106*(E12), 32,815–32,827.